



UNIVERSITÀ  
DEGLI STUDI  
FIRENZE

## FLORE

# Repository istituzionale dell'Università degli Studi di Firenze

### **Small-angle neutron scattering of mixed ionic perfluoropolyether micellar solutions**

Questa è la Versione finale referata (Post print/Accepted manuscript) della seguente pubblicazione:

*Original Citation:*

Small-angle neutron scattering of mixed ionic perfluoropolyether micellar solutions / C.M.C.Gambi; R.Giordano; A.Chittofrati; R.Pieri; M.Laurati; P.Baglioni; J.Teixeira. - In: JOURNAL OF PHYSICAL CHEMISTRY. B, CONDENSED MATTER, MATERIALS, SURFACES, INTERFACES & BIOPHYSICAL. - ISSN 1520-6106. - STAMPA. - 111:(2007), pp. 1348-1354.

*Availability:*

This version is available at: 2158/347219 since:

*Terms of use:*

Open Access

La pubblicazione è resa disponibile sotto le norme e i termini della licenza di deposito, secondo quanto stabilito dalla Policy per l'accesso aperto dell'Università degli Studi di Firenze (<https://www.sba.unifi.it/upload/policy-oa-2016-1.pdf>)

*Publisher copyright claim:*

(Article begins on next page)

## Small-Angle Neutron Scattering of Mixed Ionic Perfluoropolyether Micellar Solutions

C. M. C. Gambi,<sup>\*,†,‡</sup> R. Giordano,<sup>‡</sup> A. Chittofrati,<sup>§</sup> R. Pieri,<sup>§</sup> M. Laurati,<sup>⊥,¶</sup> P. Baglioni,<sup>||</sup> and J. Teixeira<sup>#</sup>

Department of Physics, University of Florence and CNISM, v. G. Sansone 1, 50019 Sesto Fiorentino, Firenze, Italy, Department of Physics, University of Messina and CNISM, Salita Sperone 31, 98010 S. Agata, Messina, Italy, Solvay Solexis, Research & Technology, Physical Chemistry of Interfaces, viale Lombardia 20, 20021 Bollate, Milano, Italy, Physik der Weichen Materie IPkM, Universität Heinrich-Heine Düsseldorf, Universitätsstrasse 1, 40225 Düsseldorf, Germany, Department of Chemistry, University of Florence and C.S.G.I., v. della Lastruccia 3, 50019 Sesto Fiorentino, Firenze, Italy, Laboratoire Léon Brillouin, CEA-CNRS Saclay, 91191 Gif sur Yvette Cédex, France, and INFN-CRS-Soft Matter (CNR), Università Roma "La Sapienza", P. A. Moro 2, I-00185, Roma, Italy

Received: September 18, 2006; In Final Form: December 12, 2006

Aqueous mixed micellar solutions of perfluoropolyether carboxylic salts with ammonium counterions have been studied by small-angle neutron scattering. Two surfactants differing in the tail length were mixed in proportions  $n_2/n_3 = 60/40$  w/w, where  $n_2$  and  $n_3$  are the surfactants with two and three perfluoroisopropoxy units in the tail, respectively. The tails are chlorine-terminated. The mixed micellar solutions, in the concentration range 0.1–0.2 M and thermal interval 20–40 °C, show structural characteristics of the interfacial shell that are very similar to ammonium  $n_2$  micellar solutions previously investigated; thus, the physics of the interfacial region is dominated by the polar head and counterion. The shape and dimensions of the micelles are influenced by the presence of the  $n_3$  surfactant, whose chain length in the micelle is 2 Å longer than that of the  $n_2$  surfactant. The  $n_3$  surfactant favors the ellipsoidal shape in the concentration range 0.1–0.2 M with a 1/2 ionization degree of  $n_2$  micelles. The very low surface charge of the mixed micelles is attributed to the increase in hydrophobic interactions between the surfactant tails, due to the longer  $n_3$  surfactant molecules in micelles. The closer packing of the tails decreases the micellar curvature and the repulsions between the polar heads, by surface charge neutralization of counterions migrating from the Gouy–Chapman diffuse layer, leading to micellar growth in ellipsoids with greater axial ratios.

### 1. Introduction

Perfluoropolyether (PFPE) carboxylic salts form a wide range of self-association structures in water, from liquid crystals<sup>1–3</sup> to microemulsions<sup>4–8</sup> and micellar solutions.<sup>3,9–13</sup> In the past years, a study of aqueous micellar solutions based on a high-purity PFPE carboxyl acid,  $\text{Cl}(\text{C}_3\text{F}_6\text{O})_n\text{CF}_2\text{COOH}$ , with  $n = 2$ , terminated with chlorine and with two perfluoroisopropoxy units in the tail ( $n_2$ ), has been performed by small-angle neutron scattering (SANS)<sup>14–16</sup> to characterize the micellar structure and the intermicellar interactions. Several  $n_2$  ionic surfactants with counterions with different molecular weights have been studied at different concentrations and temperatures.

In this paper, mixed micelles composed of  $n_2$  and  $n_3$  ammonium surfactants of the same high purity grade are investigated. The  $n_3$  surfactant differs from the  $n_2$  by the tail length that is composed of three perfluoroisopropoxy units ( $n = 3$ , in the formula above). The use of surfactant mixtures rather than single surfactants in the industrial utilization of surfactants

often improves performances and stability of the products. Because the mixed micelles are less known than the single surfactant micelles, basic research on mixed micelles is an important motivation for this work. In this paper,  $n_2n_3$  ammonium micellar solutions with a ratio of  $n_2/n_3 = 60/40$  w/w between the  $n_2$  and  $n_3$  surfactants have been studied by SANS at different concentrations and temperatures. These micellar solutions have been also investigated<sup>7,13</sup> by phase diagram, surface tension, and NMR.

The SANS results of the  $n_2$  ammonium micelles are reported in refs 14 and 15. The  $n_2$  micelles at 28 and 40 °C, in the surfactant concentration range from 0.05 to 0.12 M, display spherical shapes with an inner core radius of 15 Å and interfacial layer thickness of 4 Å. At 0.2 M concentration, prolate ellipsoidal micelles are observed, with axial ratio  $\sim 2$  and minor axis 13 Å. The average aggregation numbers and the surface charges lead to ionization degrees spanning from 0.3 to 0.5 in the concentration and temperature intervals investigated.

### 2. Modeling Micelles

The scattered neutron cross section per unit volume of the sample was measured vs the momentum transfer,  $Q$ . The mixed micellar solution is assumed to be composed of surfactant molecules at the critical micellar concentration, cmc, with a ratio  $n_2/n_3 = 60/40$  w/w between the  $n_2$  and  $n_3$  surfactants in the aqueous phase and micelles with an average surfactant aggregation number,  $N$ , with an effective micellar charge  $Q^*$ . In

\* Corresponding author.

† Department of Physics, University of Florence and CNISM.

‡ University of Messina and CNISM.

§ Solvay Solexis.

⊥ Universität Heinrich-Heine Düsseldorf.

|| University of Florence and C.S.G.I.

# Laboratoire Léon Brillouin, CEA-CNRS Saclay.

†† Università Roma "La Sapienza".

¶ On leave from Institut für Festkörperforschung–Forschungszentrum Jülich.

**TABLE 1: Molecular Weight (MW), Measured Density ( $d$ ) at 28 °C, Molecular Volume ( $V_m$ ), and Tail Volume ( $V_t$ ) of the n2, n3 and n2n3 Acids and Salt<sup>a</sup>**

	MW	$d$ (g/cm <sup>3</sup> )	$V_m$ (Å <sup>3</sup> )	$V_t$ (Å <sup>3</sup> )
n2-acid	462	1.809	424	387
n3-acid	628	1.845	565	528
n2n3-acid	517	1.823	471	434
n2n3-salt	534	1.837	483	434

<sup>a</sup> The ratio of n2 to n3 is 60/40 wt/wt.

addition, for the mixed micelles, we assume that the ratio n2/n3 = 60/40 w/w is maintained in the micellar core at the surfactant concentrations of 0.1 and 0.2 M of this paper.

To define the normalized particle form factor  $P(Q)$ , mixed micelles have been modeled as two-shell particles, formed of a core containing the surfactant n2n3 tails and interfacial layer containing the CO<sub>2</sub><sup>-</sup> surfactant polar head groups, some ammonium counterions NH<sub>4</sub><sup>+</sup>, and hydration water molecules. As in refs 14–16, a net separation between the fluorinated and the hydrogenated region of the micelle was assumed on the basis of the high hydrophobicity of fluorinated molecules.<sup>17</sup> For the particle form factor  $P(Q)$  of mixed micelles, we used ellipsoidal shapes and spherical shapes as detailed in ref 15.

The interparticle structure factor  $S(Q)$  is the result of steric repulsion and screened Coulombic repulsion between micelles,<sup>18–21</sup> and it has been calculated assuming an analytical solution for the multicomponent ionic liquid with a mean spherical approximation.<sup>22–24</sup> The multicomponent system was reduced to a generalized one-component macroion system.<sup>25–26</sup> A detailed description of the theoretical framework is reported in refs 27–29. According to theory, the total neutron cross section per unit volume of the sample can be written<sup>29</sup>

$$I(Q) = C_M N \sum_i b_i - V_m \rho_s)^2 P(Q) S(Q) + I_{\text{back}}$$

where  $C_M$  is the number density of the surfactant molecules in micelles ( $C_M = C - \text{cmc}$ ; with  $C$ , the surfactant concentration, and  $\text{cmc}$ , the critical micellar concentration);  $N$  is the average surfactant aggregation number of the micelle (already defined);  $\sum_i b_i$  is the total scattering length of all the atoms in the surfactant molecule;  $V_m$  is the surfactant molecule volume, or monomer volume; and  $\rho_s$  is the scattering density of the solvent, that is, the H<sub>2</sub>O scattering length divided by the H<sub>2</sub>O molecule volume. The spectrum background,  $I_{\text{back}}$ , is due to the incoherent contribution of the atoms. The term  $\sum_i b_i - V_m \rho_s$  represents the contrast,  $K$ , that is, the difference between the scattering length of the dry surfactant molecule and the solvent molecules of equivalent volume. The scattering length density of the two parts of a micelle,  $\rho_1$  (that of the hydrophobic core) and  $\rho_2$  (that of the shell), have been evaluated as reported in ref 15.

In Table 1, the molecular weight (MW); the measured density,  $d$ , at 28 °C; the molecular volume,  $V_m$ ; and the tail volume,  $V_t$ , of the n2, n3, and n2n3 acids and n2n3 ammonium surfactant (salt) are reported. We treat the n2n3 surfactant as a single surfactant composed of one head and a tail with a number of perfluoroisopropoxy units,  $n = 2.33$ , that has been calculated as follows. The volume of each molecule is obtained by the molecular weight and density  $V = \text{MW}/(dN_A)$ , where  $N_A$  is Avogadro's number; the tail volume is obtained after subtraction of the head volume from the molecular volume. The head is composed of the CO<sub>2</sub><sup>-</sup> group and the hydrogen atom for the acids or the CO<sub>2</sub><sup>-</sup> group and counterion for the surfactant. Assuming a linear trend between the tail volumes corresponding to  $n = 2$  and  $n = 3$  acids, an average value of  $n = 2.33$  for the n2n3 acid tail is evaluated.

**TABLE 2: Molecular Weight (MW), Volume ( $V$ ), Scattering Length (sl) and Scattering Length Density (sld) of Tail, Polar Head, Ammonium Counterion, and Solvent**

	MW	$V$ (Å <sup>3</sup> )	sl (10 <sup>-12</sup> cm)	sld (10 <sup>10</sup> cm <sup>-2</sup> )
tail	472	434	16.65	3.836
CO <sub>2</sub> <sup>-</sup>	44	35.26	1.826	5.179
NH <sub>4</sub> <sup>+</sup>	18	13.58	-0.566	-4.168
H <sub>2</sub> O	18	29.9	-0.1677	-0.5609

The values of MW, volume, scattering length (sl), and scattering length density (sld) of the n2n3 tail, the CO<sub>2</sub><sup>-</sup> group, the ammonium counterion,<sup>30</sup> and water are reported in Table 2. A detailed description of the spherical and ellipsoidal form factors  $P(Q)$ , of the interparticle structure factor  $S(Q)$  and of the interaction potential,  $U$ , that have been used to fit the data is reported in ref 15. The macroion structure factor was calculated using a revised version of the Hayter–Penfold Fortran package.<sup>18</sup>

The free-fitting parameters  $Q^*$ ;  $N$ ; ellipsoidal short axis,  $b$ ; and interfacial shell thickness,  $t$ , are evaluated by the fitting procedure of the above  $I(Q)$  equation to the spectrum experimental data. Other important parameters are calculated by these, that is, the fractional ionization  $\alpha = Q^*/N$  that represents the number of free counterions surrounding each micelle (i.e., the number of unscreened surfactant head groups of a micelle), the axial ratio  $a/b$  (where the long axis is calculated by the relationship  $a = 3NV_1/4\pi b^2$  where  $V_1 = 434 \text{ Å}^3$  is the surfactant tail volume reported in Table 1). Additionally calculated are the number of interfacial water molecules for the surfactant molecule,  $N_S$  (or hydration number per surfactant molecule); the average diameter,  $D$ , of the ellipsoidal micelles (or diameter of a sphere with the same volume of the ellipsoid); the Debye's length,  $l_D$ ; the contact potential,  $U_1$ ; and the volume fraction of micelles,  $\eta$  (see ref 15 for details).

### 3. Materials

The salts of ammonium (NH<sub>4</sub><sup>+</sup>) carboxylic acid (PFPE type with two or three perfluoroisopropoxy units in the hydrophobic tail) were provided by Solvay Solexis, Milan, Italy, with purity of 99.8% for the n2 surfactant and 99.5% for the n3 one.<sup>7,13</sup> The molecular weight of the acids obtained by titration and NMR agreed within 5% experimental error with the calculated value. The dry surfactants, prepared by neutralizing the acid with a stoichiometric amount of the corresponding hydroxide, were free of acid and inorganic impurities within analytical sensitivities. All the solutions were prepared using Milli-Q water.

The critical micellar concentration of n3 micelles is  $0.96 \times 10^{-3} \text{ M}$  at 25 °C and that of the mixed micelles is  $2.8 \times 10^{-3} \text{ M}$  at 25 °C as obtained by equilibrium surface tension measurements (accuracy 8%) using the Du Nouy method by a Lauda TEIC tensiometer connected to a thermostatic bath and applying to the raw force data the Harkins–Jordan correction factor. A negligible variation of the cmc has been observed up to 40 °C. The cmc of n2 micelles was 0.021 M by surface tension;<sup>7</sup> thus, the cmc of mixed micelles is intermediate between that of n2 and n3 micelles.

Liquid crystal formation in the aqueous n3 and n2 micelles has been observed<sup>7,13</sup> above 1–2% w/w and 25% w/w surfactant concentration, respectively at 25 °C. All the micellar solutions were macroscopic single isotropic phases and were individually checked for invariance upon aging or centrifugation. The n3 micellar solution with surfactant concentration 0.60% w/w has been studied in this work. The molecular weight of the ammonium n3 surfactant is 645.

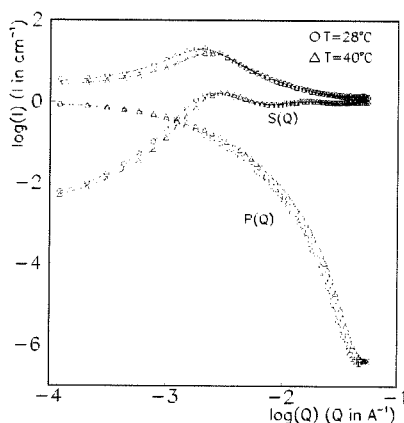


**Figure 1.** Experimental scattered intensity,  $I$  ( $\text{cm}^{-1}$ ), vs  $Q$  ( $\text{\AA}^{-1}$ ) of ammonium mixed micellar solutions at 0.1962 M concentration and temperatures of 28 (circles) and 40 °C (triangles). Continuous lines are the fitted curves. The corresponding normalized form  $P(Q)$  and structure  $S(Q)$  factors are reported in the bottom part of the figure for each sample (symbols as above connected by dashed and continuous lines, respectively). The vertical scale of the normalized form and structure factors is dimensionless. The error bars (standard deviation) are drawn, except when they are smaller than the symbol used.

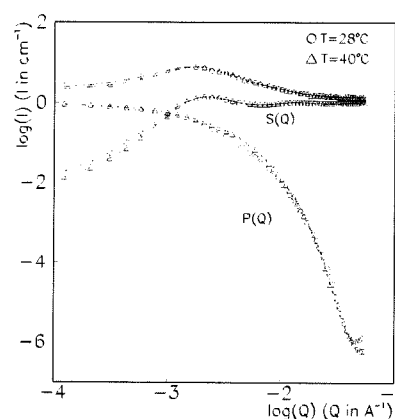


**Figure 2.** Experimental scattered intensity,  $I$  ( $\text{cm}^{-1}$ ), vs  $Q$  ( $\text{\AA}^{-1}$ ) of ammonium mixed micellar solutions at 0.09582 M concentration and temperatures of 28 (circles) and 40 °C (triangles). Continuous lines are the fitted curves. The corresponding normalized form  $P(Q)$  and structure  $S(Q)$  factors are reported in the bottom part of the figure for each sample (symbols as above connected by dashed and continuous lines, respectively). The vertical scale of the normalized form and structure factors is dimensionless. The error bars (standard deviation) are drawn, except when they are smaller than the symbol used.

The density values reported in Table 1 were measured by a PAAR DMA 5000 density meter at  $28 \pm 0.1$  °C.

#### 4. Method

SANS experiments on n2n3 micelles were performed at the PAXE spectrometer (Lab. Léon Brillouin, Saclay) with a sample–detector distance of 2.56 m and 5 Å incident neutron wavelength with a wavelength spread of  $\pm 5\%$ . Collimation was achieved by two slits of 12 and 7 mm diameter, placed 2.5 m apart. The two-dimensional intensity distributions were corrected for the background and the empty cell contributions and then normalized to absolute intensity by a direct measurement of the intensity of the incident neutron beam.<sup>27,31</sup> By integrating the normalized two-dimensional intensity distribution with respect to the azimuthal angle, one-dimensional scattering intensity distributions,  $I(Q)$ , in the unit of a differential cross section per unit volume ( $\text{cm}^{-1}$ ) were obtained.

SANS and ultra-SANS (USANS) experiments on n3 micelles were performed using the KWS-1 and KWS-3 spectrometers (Forschungszentrum Jülich) in the  $Q$  range  $3 \times 10^{-3}$  to  $3.8 \times 10^{-2}$   $\text{\AA}^{-1}$  and  $2 \times 10^{-5}$  to  $2.5 \times 10^{-3}$   $\text{\AA}^{-1}$ , respectively. On the spectrometer KWS-1, the incident neutron wavelength was 7 Å with a wavelength spread of  $\pm 10\%$ , and data were measured at sample–detector distances of 2, 8, and 20 m, with respective collimations of 8, 8, and 20 m. Data were corrected for the background and the empty cell contributions and normalized to absolute intensity by measuring the scattering cross section of a plexiglass standard. The spectrometer KWS-3 was used in pinhole geometry with incident neutron wavelength of 12.7 Å (wavelength spread of 9% at fwhm). Data were corrected and normalized to absolute units with respect to the scattered intensity of the incident neutron beam.

Samples were contained in flat quartz cells of 1 mm thickness and measured at 28 and 40 °C with a thermal stability of  $\pm 0.1$  °C.

#### 5. Results

**Mixed Micelles.** The experimental spectra of mixed n2n3 micellar solutions with surfactant concentrations of  $C = 0.2$  and 0.1 M are plotted in Figures 1 and 2 at 28 and 40 °C,

respectively.  $I(Q)$ , the scattered neutron cross section per unit volume of the sample, is reported vs the momentum transfer  $Q$ . The spectra are characterized by a sharp structural peak, which is a manifestation of strong interactions between the micelles. By comparison of Figures 1 and 2, the decrease in concentration leads to a decrease in the peak intensity for both temperatures. The fitting procedure of the experimental data to the theoretical model has been performed for the samples in the explored thermal range. In Figures 1 and 2, the fitted curves (continuous lines) and the form and structure factors (dashed and continuous lines, respectively) are reported for each sample. The model that fits the experimental spectra is the ellipsoidal model for both concentrations and temperatures. The model of polydispersed spheres did not fit the spectra. We have to point out that ellipsoids with axial ratios close to 1 are equivalent to spheres. However, this is not our case because the axial ratios found are in the range 2.4–3 (see Table 3).

From the results, the mixed micelles are prolate ellipsoids. The free-fitting parameters  $Q^*$ ,  $N$ ,  $t$ , and  $b$  are evaluated for the samples studied and are reported in Table 3. In addition to the free-fitting parameters, for all the samples, Table 3 reports some other parameters calculated by the previous ones, that is, the fractional ionization,  $\alpha$ ; the axial ratio,  $a/b$ ; the hydration number,  $N_S$ ; the average diameter,  $D$ , of the ellipsoidal micelles; the Debye's length,  $l_D$ ; the contact potential,  $U_1$ ; and the volume fraction of micelles,  $\eta$ . Furthermore, in Table 4, the inner (core–shell) and outer (micelle–solvent) surface per polar head are calculated from the geometrical parameters ( $b$ ,  $a$ , and  $t$ ) and  $N$  of Table 3.  $\Sigma_{\text{inner}}$  is also called surfactant area per polar head.

To evaluate the accuracy of the parameters of Table 3, for each spectrum, several fits have been done, changing the initial numerical values of the four free fitting parameters,  $Q^*$ ,  $N$ ,  $t$ , and  $b$ , to maintain the same good quality of the reduced  $\chi^2$  values. Each parameter (with the other three fixed) is given slightly different values (about 10 values) to find out the range of variability that does not degrade the quality of the reduced  $\chi^2$ . The values of the parameters of Table 3 are average values. The error on the free-fitting parameters is obtained as a percentage of the maximum difference from the average value. The error in the other parameters of Table 3 and those of Table 4 is calculated by the error propagation procedure.



**TABLE 3: SANS Results of n2n3 PFPE Ionic Micellar Solutions with NH<sub>4</sub><sup>+</sup> Counterions at Temperatures of 28 and 40 °C<sup>a</sup>**

<i>C</i> (M)	<i>Q</i> <sup>*</sup>	<i>N</i>	<i>t</i> (Å)	<i>b</i> (Å)	$\alpha$	<i>D</i> (Å)	<i>a/b</i>	<i>N<sub>s</sub></i>	<i>l<sub>D</sub></i> (Å)	<i>U<sub>1</sub></i> (kBT)	$\eta$	$\chi^2$
28 °C												
0.1962	16.4	117	3.85	17.0	0.140	54.4	2.89	8.0	24.2	7.60	0.0839	1.0
0.09582	13.3	83.0	3.82	15.4	0.160	49.1	2.35	8.9	30.1	7.76	0.0418	1.0
40 °C												
0.1962	16.3	94.8	3.86	15.4	0.171	51.2	2.68	8.8	22.3	7.65	0.0864	1.0
0.09582	15.1	75.7	3.86	16.4	0.200	47.7	1.78	9.0	28.3	9.65	0.0420	1.0

<sup>a</sup> *C* is the molar surfactant concentration; *Q*<sup>\*</sup>, the effective charge; *N*, the average aggregation number; *t*, the micellar shell thickness; *b*, the micellar inner minor axis;  $\alpha$ , the fractional ionization; *D*, the diameter of the equivalent spherical micelle; *a/b*, the axial ratio with *a* major axis of the micelle; *N<sub>s</sub>*, the hydration number; *l<sub>D</sub>*, the Debye's length; *U<sub>1</sub>*, the potential on the micellar surface;  $\eta$ , the volume fraction of the micelles; and the reduced  $\chi^2$ .

**TABLE 4: Inner and Outer Surface Per Polar Head Group Calculated from the Results Reported in Table 3**

<i>C</i> (M)	$\Sigma_{\text{inner}}$ (Å <sup>2</sup> )	$\Sigma_{\text{outer}}$ (Å <sup>2</sup> )
28 °C		
0.1962	74	111
0.09582	71	110
40 °C		
0.1962	70	109
0.09582	69	106

The accuracy of *Q*<sup>\*</sup> and *N* is 3%; thus,  $\alpha$  is known with 6% accuracy. The thickness, *t*, is known with 10% accuracy; short axis, *b*, and diameter, *D*, with 2%; axial ratio *a/b* with 4%;  $\Sigma_{\text{inner}}$  with 5%; and  $\Sigma_{\text{outer}}$  with 11% accuracy. The quality of each fit was deduced by the reduced  $\chi^2$  value, which is always 1, as shown in Table 3.

**n3 Micelles.** As reported in the Materials section, aqueous n3 micellar solutions exist in the concentration range between  $\text{cmc} = 0.96 \times 10^{-3}$  M and the threshold of liquid crystal formation, 0.015–0.030 M (1–2% w/w).<sup>7</sup> The n3 micellar solution SANS spectra with  $C = 9.3 \times 10^{-3}$  M (0.60% w/w) at 28 °C (PAXE spectrometer) and 40 °C (KWS1 spectrometer) are reported in Figures 3a and 4a, respectively. This concentration was chosen because it is below the liquid–crystal threshold (~0.015 M) and one of the closer to the lower concentration studied for mixed micelles, ~0.1 M. The n3 spectra are very different from n2 and n2n3 spectra. In fact, no structural peak is shown. To ascertain the nature of the intensity increase at low *Q*, we performed an USANS experiment at 40 °C. This spectrum is reported in Figure 5 in a log–log plot together with the SANS spectrum of Figure 4a, at the same temperature, to compare the trend of the scattered intensity on the whole *Q* range. The trend is the same. The measurement on the USANS *Q* range was done only for the sample at 40 °C because we suspect that at 28 °C, the sample is below the Krafft point. In fact, it is very difficult to detect a few aggregates. In the previous literature, for the n2 ammonium surfactant, the Krafft point was found at 10–15 °C by conductivity studies;<sup>9</sup> the n3 surfactant has very low solubility at 25 °C;<sup>13</sup> and for the n4 ammonium surfactant (composed of 4 perfluoroisopropoxy units in the tail), the temperature of 25 °C was found to be below the Krafft point.<sup>12</sup> Thus, at 28 °C, the n3 ammonium surfactant can be below the Krafft point.

All the spectra of the n3 sample show an important intensity increase at low *Q*. No structural peak is observed, and no pure form factor trend is shown. However, we tried to analyze the spectra by means of the theory described above for mixed micelles and also by using only form factors (polydispersed spheres, ellipsoids, disks, and cylinders) without success. Furthermore, for the 40 °C SANS spectrum, very large micelles of 500–600 Å size can be found by fitting the experimental points at low *Q* to the Guinier law<sup>31</sup> or the whole spectrum to

a cylindrical form factor.<sup>32</sup> However, this size is incompatible with the length of the n3 surfactant molecule (that is, 13 Å in liquid crystal lamellar phases<sup>13</sup>) and with the *b* values of the mixed n2n3 micelles of this work. *b* is strictly related to the surfactant chain length; thus, taking into account that the sample is close to the liquid–crystal phase transition border, we have done the hypothesis that large concentration fluctuations influence the physics of the sample. We have used the Ornstein–Zernike (OZ) equation  $I(Q) \sim 1/(1 + (Q\xi)^2)$  (where  $\xi$  represents the correlation length of the concentration fluctuations<sup>31</sup>) to see if a  $1/I(Q)$  vs  $Q^2$  plot shows a straight line trend (see Figures 3b, 4b, and 5b for the SANS spectrum at 28 °C, SANS, and USANS spectra at 40 °C, respectively). In Figures 3b and 4b, the scattering seems due to a mixture of concentration fluctuations and particles in solution. In fact, no clear linear trend is shown. The fit of Figure 5b follows the OZ equation in the whole *Q* range, with a  $\xi = 533 \pm 40$  Å and  $\chi^2 = 1$ . Large concentration fluctuations are detected in this case. The presence of concentration fluctuations is in agreement with the results obtained from fluorescence quenching;<sup>11</sup> i.e., n3 sodium micellar solutions close to cmc do not form well-organized structures, but rather, loose structures permeated with water molecules. The comparison with sodium micelles is reasonable because the phase behavior of sodium and ammonium n3 solutions is very similar, and the cmc is also very similar ( $0.57 \times 10^{-3}$  M for sodium n3 micelles to be compared with  $0.96 \times 10^{-3}$  M for ammonium ones).

## 6. Discussion

We now focus our attention on the comparison between the ammonium n2n3 and n2 micellar solutions (studied in refs 14–15) in the concentration range 0.1–0.2 M and thermal interval 28–40 °C with the aim to highlight the peculiarity of the n2n3 mixed micelles.

From the reported SANS results, n2n3 aggregates are found in solution with microstructural properties typical of ellipsoidal ionic micelles in solution. For the n2n3 system (see Table 3), the micellar inner core is defined by the short and long axes, *b* and *a*, respectively. *b* varies from 15 to 17 Å, and the axial ratio, from 3 to 2.4. The minimum *b* value, 15 Å, represents the n2n3 surfactant tail length in the micelle.

In n2 ammonium micelles,<sup>15</sup> at  $C = 0.2$  M, the micelles are prolate ellipsoids with a 13 Å short axis minimum value and axial ratio in the range 2.2–2.5, whereas at  $C = 0.1$  M, the micelles are spherical. Thus, the n3 surfactant addition to n2 micelles favors the ellipsoidal shape with greater axial ratios and *b* values 2 Å longer, that is, greater short and long axes. This increase in both the short and long axes makes it possible to suggest some hypotheses on the n3 surfactant distribution into the micelle. In fact, the n3 surfactant is composed of three perfluoroisopropoxy units in the tail, one more than the n2

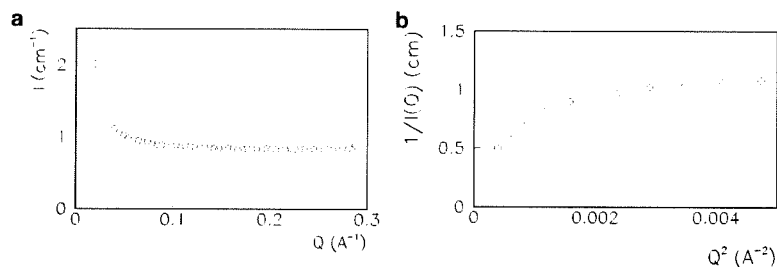


**Figure 3.** n3 SANS spectrum at 28 °C. (a) Experimental scattered intensity,  $I$  ( $\text{cm}^{-1}$ ), vs  $Q$  ( $\text{\AA}^{-1}$ ) of the ammonium n3 micellar solution at  $C = 0.0093 \times 10^{-3}$  M (0.60% w/w). (b)  $1/I(Q)$  as a function of  $Q^2$ . The error bars (standard deviation) are drawn, except when they are smaller than the symbol used.

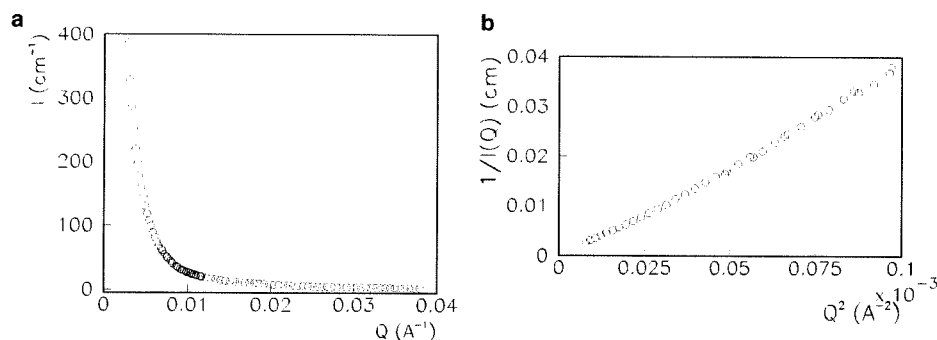


**Figure 4.** n3 SANS spectrum at 40 °C. (a) Experimental scattered intensity,  $I$  ( $\text{cm}^{-1}$ ), vs  $Q$  ( $\text{\AA}^{-1}$ ) of ammonium n3 micellar solution at  $C = 0.93 \times 10^{-5}$  M (0.60% w/w). (b)  $1/I(Q)$  as a function of  $Q^2$ . The error bars (standard deviation) are drawn, except when they are smaller than the symbol used.

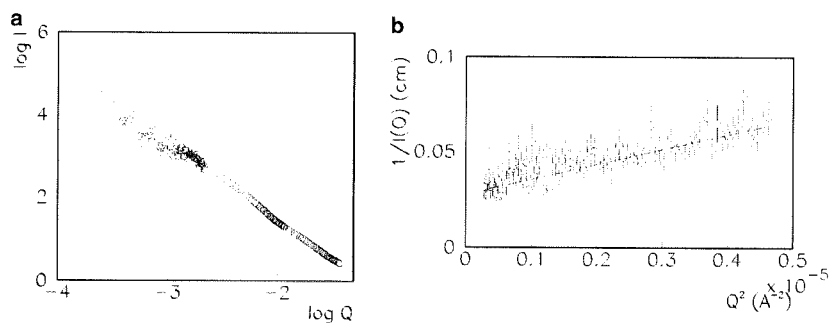


**Figure 5.** (a) USANS and SANS experimental intensity vs  $Q$  in a log–log scale for the n3 sample at  $C = 0.93 \times 10^{-5}$  M (0.60% w/w) (40°). (b)  $1/I(Q)$  as a function of  $Q^2$  of the USANS plot. The continuous line represents the best fit to the experimental points. The error bars (standard deviation) are drawn.

surfactant; thus, the n3 molecule is longer than the n2. This result suggests that the central part of the micelle, characterized by the parameter  $b$ , is composed of n2 and n3 surfactants. The composition of the end parts of the micelle is less defined. In fact, the end parts can be composed of only n3 surfactant or a mixture of n2 and n3 surfactants. Because of the 2 Å difference between the n2 and n3 surfactant lengths, it is unlikely that the end parts are composed of only n2 surfactant for reason of steric hindrance.

By  $F^{19}$  NMR technique,<sup>12</sup> for ammonium n2n3 micelles at concentration 0.1 and 0.2 M, the partition into the micelles of the n2 and n3 surfactants corresponds to almost ideal and ideal mixing, respectively, which means that the ratio n2/n3 = 60/40 w/w is maintained in 0.2 M micelles and almost maintained in 0.1 M micelles. Our hypothesis reported in the Modeling Micelles section (the n2/n3 ratio into the micelle is the same of the initial composition for the concentrations studied) was done on the basis of the  $F^{19}$  NMR results. Neither  $F^{19}$  NMR nor SANS can specify the exact partition of the n3 surfactant between the central and end parts of the micelle; however, one conclusion is clear: from the  $b$  values, the n3 surfactant in the micelle is

2 Å longer than the n2 and significantly influences the size and shape of the mixed micelles. As a consequence, the average diameter of the n2n3 micelles, 50 Å, is larger than that of the n2 micelles, 40 Å, and the micellar growth seems to follow the theory of the ladder model.<sup>33</sup> Far above the cmc, long micelles are formed with average size increasing as the surfactant concentration increases (see Table 3).

We compare our SANS results on the surfactant length with the SAXS results on the liquid crystal lamellar phase of the sodium surfactant series.<sup>13</sup> The sodium n2, n3, and n4 surfactant lengths were 10.6, 12.6, and 14.8 Å, respectively at 85% w/w surfactant concentration,<sup>13</sup> resulting in a 2 Å increase for one perfluoroisopropoxy unit addition, as found in this work by SANS between n2 and n3 surfactants. The lamellar packing obviously leads to shorter surfactant lengths than the micellar ones.

In the interfacial region, on the contrary, the influence of the n3 surfactant is negligible. In fact, the interfacial layer thickness is  $t = 3.8 \pm 0.4$  Å, as for n2 ammonium micelles,<sup>15</sup> and in the limit of the experimental errors is not affected by the n3 longer tail, confirming that the shell thickness depends mainly on the



carboxylic head and counterion. Furthermore, the area per polar head of the micellar inner and outer surfaces is  $\sim 70$  and  $\sim 110$  Å<sup>2</sup> (see Table 4), respectively, for both concentrations and temperatures. These values agree with those of n2 ammonium micelles obtained by SANS in ref 15 and with the values obtained by surface tension on the n2 and n3 surfactants ( $70\text{--}75$  Å<sup>2</sup>).<sup>3,7</sup>

In summary, the addition of n3 to n2 micellar solutions leads to prolate ellipsoidal shape in a larger concentration range 0.1–0.2 M between 28 and 40 °C, and the mixed micelles are greater than n2 micelles, whereas the interfacial regions are very similar.

The n2n3 net micellar surface charge changes slightly versus concentration and temperature in the ranges studied, with values lower than those of n2 micelles. The average aggregation number decreases vs concentration increase at constant temperature and decreases vs the temperature increase at constant concentration, as also found for n2 ammonium micelles, but with larger values for the mixed micelles.

We have to point out that for an increase of one perfluoroisopropoxy unit in the surfactant tail, the cmc decreases by a 1.5 order of magnitude and the liquid crystal threshold decreases by 1 order of magnitude (at 25 and 40 °C).<sup>7</sup> This result was interpreted in ref 7 in terms of increased hydrophobic interactions between the surfactant tails. The packing of greater tails led to less curved micellar surfaces; thus, the repulsion between the polar heads must be reduced by neutralization of some polar head charges from the counterion migration of the micellar Gouy–Chapman diffuse layer. Furthermore, because less charged micelles can grow better because of the reduced repulsion between the polar heads,  $N$  can increase, leading to higher  $a/b$  axial ratios. As a consequence, the ionization degree  $\alpha = Q^*/N$  of n2n3 micelles is lower, spanning from 0.14 to 0.20 (in n2 micelles  $\alpha$  values 0.33 and 0.40 were found at  $C = 0.2$  and 0.1 M, respectively). As a consequence of the reduced surface charge, the Debye's lengths of the mixed micelles are longer than those of n2 micelles.

## 7. Conclusion

In summary, the structure of ammonium mixed n2n3 micelles has been characterized by SANS. Interfacial shell thickness, area per polar head, and water molecules per polar head are the same as the n2 ammonium surfactant micelles; thus, the physics of the interfacial shell is influenced only by the polar head and counterion. The shape and dimension of the micelles are influenced by the presence of the n3 surfactant, whose chain length is 2 Å longer than that of the n2 surfactant. The n3 surfactant is distributed into the micelle, leading to ellipsoidal micelles in the concentration range 0.1–0.2 M, with 1/2 ionization degree of the n2 micelles. The very low surface charge that is a consequence of the greater hydrophobic interactions between the surfactant tails leads to micelles that can grow in an ellipsoidal shape with greater axial ratios.

**Acknowledgment.** We thank S. Fontana and C. Tonelli for the thorough purification of the materials. We also thank J. Stellbrink for helpful discussion and for USANS measurements. Acknowledgments are due to EC for support via the NMI3 Programme (Contract no. RII3-CT-2003-505925) and to MURST (PRIN 2003 and PRIN 2005), INFM, and CSGI for financial support.

## References and Notes

(1) Wurtz, J.; Meyer, J.; Hoffmann, H. *Phys. Chem. Chem. Phys.* **2001**, *3* (15), 3132.

- (2) Caboi, F.; Chittofrati, A.; Monduzzi, M.; Morioni, C. *Langmuir* **1996**, *12*, 6022–6027.
- (3) Caboi, F.; Chittofrati, A.; Lazzari, P.; Monduzzi, M. *Colloids Surf. A* **1999**, *160*, 47.
- (4) Baglioni, P.; Gambi, C. M. C.; Giordano, R.; Senatra, D. *J. Mol. Struct.* **1996**, *383*, 165–169.
- (5) Baglioni, P.; Gambi, C. M. C.; Giordano, R. *Physica B* **1997**, *234–236*, 295–296.
- (6) Monduzzi, M.; Knacksted, M. A.; Ninham, B. W. *J. Phys. Chem.* **1995**, *99*, 17772.
- (7) Chittofrati, A.; Pieri, R.; D'Aprile, F.; Lenti, D.; Maccone, P.; Visca, M. *Progr. Colloid Polym. Sci.* **2004**, *123*, 23.
- (8) Mele, S.; Chittofrati, A.; Ninham, B. W.; Monduzzi, M. *J. Phys. Chem. B* **2004**, *108* (24), 8201–8207.
- (9) Kallay, N.; Tomisic, V.; Hrust, V.; Pieri, R.; Chittofrati, A. *Colloid Surf. A* **2003**, *222*, 95.
- (10) Sulak, K.; Szajdzinska-Pietek, E. In *Proceedings of the Conference Surfactants and Dispersed Systems in Theory and Practice*, Soruz, Polanica Zdroj, May 20–23; Wilk, K. A., Ed.; Oficyna Wydawnicza Politechniki Wroclawskiej: Wroclaw, Poland, 2003.
- (11) Sulak, K.; Wolszczak, M.; Chittofrati, A.; Szajdzinska-Pietek, E. *J. Phys. Chem. B* **2005**, *109*, 799.
- (12) Mele, S.; Murgia, S.; Monduzzi, M. *J. Fluorine Chem.* **2004**, *125*, 261–269.
- (13) Mele, S.; Ninham, B. W.; Monduzzi, M. *J. Phys. Chem. B* **2004**, *108*, 17751.
- (14) Gambi, C. M. C.; Giordano, R.; Chittofrati, A.; Pieri, R.; Baglioni, P.; Teixeira, J. *J. Appl. Phys. A* **2002**, *74* (Suppl.), 5436.
- (15) Gambi, C. M. C.; Giordano, R.; Chittofrati, A.; Pieri, R.; Baglioni, P.; Teixeira, J. *J. Phys. Chem. A* **2003**, *107*, 11558.
- (16) Gambi, C. M. C.; Giordano, R.; Chittofrati, A.; Pieri, R.; Baglioni, P.; Teixeira, J. *J. Phys. Chem. B* **2005**, *109*, 8592.
- (17) Kissa, E. *Fluorinated Surfactants*; Surfactant Science Series 50; Marcel Dekker: New York, 1994.
- (18) Hayter, J. B.; Penfold, J. J. *J. Mol. Phys.* **1981**, *42*, 109.
- (19) Hayter, J. B.; Penfold, J. J. *J. Chem. Soc. Faraday Trans.* **1981**, *77*, 1851.
- (20) Snook, I. K.; Hayter, J. B. *Langmuir* **1992**, *8*, 2880–2884.
- (21) Hunter, R. J. *Foundation of Colloid Science*; Oxford Science Publications; Clarendon Press: Oxford, England; Oxford University Press: New York, 1989; Vol. 2, Chapter 14.
- (22) Hansen, J. P.; Hayter, J. B. *Mol. Phys.* **1982**, *46*, 651–656.
- (23) Sheu, E. Y.; Wu, C. F.; Chen, S.-H.; Blum, L. *Phys. Rev. A* **1985**, *32*, 3807.
- (24) Senatore, G. In *Structure and Dynamics of Strongly Interacting Colloids and Supramolecular Aggregates in Solutions*; Chen, S.-H., Huang, J. S., Tartaglia, P., Eds.; Kluwer Academic Publishers: Dordrecht, The Netherlands, 1992; pp 175–189.
- (25) Chen, S.-H.; Sheu, E. Y. In *Micellar Solutions and Microemulsions. Structure, Dynamics, and Statistical Thermodynamics*; Chen, S.-H., Rajagopalan, R., Eds.; Springer-Verlag: New York, 1990; pp 3–28.
- (26) Chen, S.-H.; Sheu, E. Y.; Kalus, J.; Hoffmann, H. *J. Appl. Crystallogr.* **1988**, *21*, 751.
- (27) Liu, Y. C.; Baglioni, P.; Teixeira, J.; Chen, S.-H. *J. Phys. Chem.* **1994**, *98*, 10208.
- (28) Liu, Y. C.; Ku, C. K.; Lo Nostro, P.; Chen, S.-H. *Phys. Rev. E* **1995**, *51*, 4598.
- (29) Sheu, E. Y.; Chen, S.-H.; Huang, J. S. *J. Phys. Chem.* **1987**, *91*, 1535.
- (30) Yizhak, Marcus. *Ion Properties*; Marcel Dekker: New York, 1997; p 46.
- (31) Teixeira, J. In *Structure and Dynamics of Strongly Interacting Colloids and Supramolecular Aggregates in Solutions*; Chen, S.-H., Huang, J. S., Tartaglia, P., Eds.; Kluwer Academic Publisher: Dordrecht, The Netherlands, 1992; pp 635–658.
- (32) Giordano, R.; Migliardo, P.; Wanderlingh, U.; Bardez, E.; Vasi, C. *J. Mol. Struct.* **1993**, *296*, 265.
- (33) Missel, P. J.; Mazer, N. A.; Benedek, G. B.; Young, Y.; Carey, M. C. *J. Phys. Chem.* **1980**, *84*, 1044.